A Neutron Activation Analysis Facility for *in vivo* Measurement of Nitrogen and Chlorine in Children

Daniel J. Borovnicar[1,3], Daniel B. Stroud[1,2], Mark L. Wahlqvist[3] and Boyd J. G. Strauss[1]

1. *Body Composition Laboratory, Monash Medical Centre, the*
2. *Department of Medical Physics, Monash Medical Centre, and the*
3. *Department of Medicine, Monash University, Clayton, Melbourne, Victoria 3168, Australia.*

Abstract

The construction, calibration and evaluation of a prompt-γ *in vivo* neutron activation analysis (IVNAA) facility for the simultaneous measurement of total body nitrogen (TBN) and chlorine (TBCl) in children is described. Subjects are irradiated unilaterally by a 0.2 GBq ^{252}Cf neutron source from shoulder to mid thigh in both supine and prone positions. Prompt γ-ray spectra are measured with two pairs of NaI(Tl) crystals (each crystal: 10 cm × 10 cm × 15 cm) positioned on both sides of the subject. TBN and TBCl are estimated from the ratios of nitrogen-to-hydrogen (N_c/H_c) and chlorine-to-hydrogen (Cl_c/H_c) counts as determined from the measurement of 10.83 MeV, 8.57 MeV and 2.22 MeV prompt γ-rays from the respective reactions $^{14}N(n,\gamma)^{15}N$, $^{35}Cl(n,\gamma)^{36}Cl$, and $^{1}H(n,\gamma)D$. N_c/H_c and Cl_c/H_c are corrected for the effect of body width and thickness on background and γ-ray attenuation. Total body hydrogen (TBH) is used as an internal standard which is independently determined using a four compartment model of body weight defined as the sum of total body water (TBW) measured by the D_2O dilution technique, total body protein (TBPr) (i.e. 6.25 x TBN) measured by IVNAA, total body bone mineral (TBBM) measured by dual energy x-ray absorptiometry and total body fat (TBF) estimated as body weight less the sum of TBW, TBPr and TBBM. The effective dose equivalent to a small child is 0.25 mSv (Q=20) per measurement scan. Repeated measurements of a child-size bottle phantom containing tissue-equivalent concentrations of nitrogen and chlorine yield respective intra- and inter-assay precision values of 2.8% (CV) and 2.3% for TBN measurements, and 7.9% and 10.0% for TBCl measurements. Similarly, intra- and inter-assay accuracy is determined to be respectively +0.1% ±1.0% (mean, 95% confidence interval) and +1.4% ±1.4% for TBN measurements, and +2.3% ± 4.3% and +3.9% ±6.0% for TBCl measurements.

Key Words

in vivo neutron activation analysis, IVNAA, nitrogen, chlorine, children

Introduction

Protein-energy malnutrition (PEM) is a common sequela in children experiencing chronic conditions such as cystic fibrosis[1] and renal failure.[2] At a systemic level, PEM may be characterised by total body protein (TBPr) depletion and relative changes in extra-cellular water (ECW).[3] Objective measurement of TBPr and ECW therefore provides a useful approach to the diagnosis and monitoring of underlying disturbances in nutritional status that may otherwise be undetected by more traditional measurements of weight and height.[4]

Received 3rd June 1996; accepted in final form 21st November 1996

An established method of measuring TBPr and ECW is *in vivo* neutron activation analysis (IVNAA). In brief, total body nitrogen (TBN) and chlorine (TBCl) are determined by counting neutron-induced prompt-γ rays with characteristic energies of 10.83 MeV and 8.57 MeV from the respective reactions $^{14}N(n,\gamma)^{15}N$ and $^{35}Cl(n,\gamma)^{36}Cl$.[5,6] TBPr is then calculated as 6.25 × TBN.[7] ECW is also calculated as (0.90 × 0.93 × 0.95 × TBCl mmol)/(100 mmol/litre) where approximately 90% of TBCl is distributed in ECW, 0.93 is an approximate serum water concentration, 0.95 represents the Donnan equilibrium factor, and 100 mmol/litre is an approximate plasma chloride concentration.[8,9]

A prompt-γ IVNAA facility has been installed at Monash Medical Centre (MMC), Melbourne, for the measurement of TBPr in adults. This facility has been previously described elsewhere.[10,11] Recent clinical and research interests at MMC have focused on the nutritional health of children. This has provided an opportunity to apply the IVNAA technique to

children who have relatively small masses of nitrogen and chlorine. The aim of this paper is to describe the construction, calibration and evaluation of a newly upgraded IVNAA facility for the simultaneous measurement of TBN and TBCl in children.

Internal Standardisation

Absolute estimates of TBN and TBCl are determined using total body hydrogen (TBH) as an internal standard by counting the 2.22 MeV prompt γ-rays which are emitted from the reaction $^1H(n,\gamma)D$.[12] This internal standardisation reduces the dependency of TBN and TBCl measurements on variables such as body size and position, and the distribution of nitrogen and chlorine in body tissues. At MMC, a subject's TBN is calculated from the relation

$$TBN_{sub} = TBH_{sub} \times \left[\frac{TBN_{cal}}{TBH_{cal}}\right] \times \left[\frac{(N_c/H_c)_{sub}}{(N_c/H_c)_{cal}}\right] \times A \quad (1)$$

where TBH_{sub} is an independent estimate of the subject's TBH (see 'Measurement Protocol', step 1), TBN_{cal} and TBH_{cal} are the known masses of nitrogen and hydrogen contained in the daily standard calibration phantom (see 'Measurement Protocol', step 5), $(N_c/H_c)_{sub}$ and $(N_c/H_c)_{cal}$ are respectively the subject's and calibration phantom's measured nitrogen-to-hydrogen counts ratio, and A is a γ-ray attenuation correction factor which corrects for the effect on $(N_c/H_c)_{sub}$ of a subject's departure in size from the dimensions of the calibration phantom. In practice, A is determined as

$$A = \left[\frac{(N_c/H_c)_{cal}}{(N_c/H_c)_{sub}}\right]_{phant} \quad (2)$$

where the subscript 'phant' indicates that the N_c/H_c count ratio for both the calibration phantom and the subject are estimated from separate measurements of size-equivalent bottle phantoms containing a concentrated urea solution (see 'Effect of Body Size on N_c/H_c and Cl_c/H_c Count Ratios'). In addition, the above equations are similar for the measurement of TBCl except that A is determined from size-equivalent phantoms filled with concentrated saline solution (see 'Effect of Body Size on N_c/H_c and Cl_c/H_c Count Ratios').

The Prompt- IVNAA Facility

Irradiation Geometry

Figure 1 shows a cross-sectional view of the IVNAA facility. A 0.2 GBq ^{252}Cf neutron source is positioned at the apex of an inverted, rectangular, conical void cast within a paraffin-wax block (40 cm × 40 cm × 60 cm) doped with boric acid (5% H_3BO_3 by weight). The collimator defines a rectangular neutron-beam aperture measuring 40 cm (length) × 20 cm (width) at a bed level of 50 cm above the neutron source. The patient is positioned supine on an aluminium bed which moves directly over the neutron source and through the upwardly collimated neutron beam. Lead is placed above the neutron collimator, in the shadow of the fast neutron beam, to provide a shielded platform for the NaI(Tl) detectors. Paraffin wax and sheets of lead surround the neutron collimator to provide radiation shielding for the IVNAA-facility operator.

γ Spectroscopy System

Figure 1 shows two pairs of 10 cm × 10 cm × 15 cm NaI(Tl) detectors positioned on both sides of the scanning bed along a horizontal axis perpendicular to the vertical neutron beam. Each detector is shielded from neutrons by a 2.5 cm thick borated-wax housing (5% H_3BO_3 by weight). Both detector housings are positioned 50 cm apart on a lead platform that skirts the neutron-beam aperture. Notably, this detector configuration compares favourably with the findings of Stamatelatos *et al*[13,14] and the inter-comparison of selected IVNAA facilities by McNeill *et al*[15] which suggest that measurement precision per unit of radiation dose is optimised using a detection system based on several smaller-sized NaI(Tl) detectors rather than a smaller number of larger-sized NaI(I) detectors. This is an important design criterion because children contain approximately 50% less nitrogen and chlorine than adults, and children are relatively more sensitive to the health risks associated with radiation than are adults.[16]

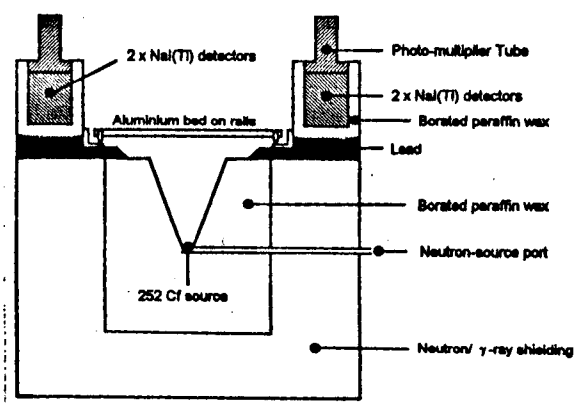

Figure 1. *A schematic diagram of the IVNAA facility at Monash Medical Centre.*

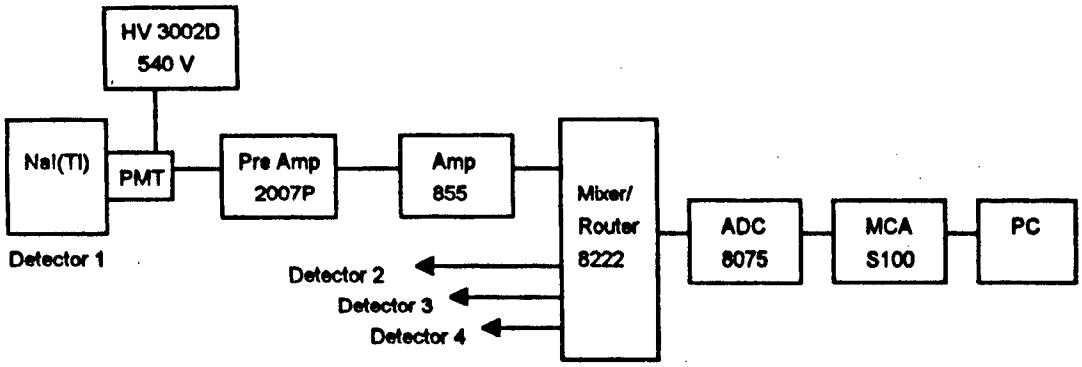

Figure 2. *A schematic diagram of the γ-spectroscopy system; PMT: photomultiplier tube; HV: high voltage; ADC: analogue-digital converter; MCA: multi-channel analyser; PC: personal computer; detection/amplification circuits for detectors 2, 3 and 4 are not shown for clarity; model numbers refer to Canberra or Ortec modules.*

Figure 2 shows a schematic diagram of the γ-spectroscopy system. Scintillations in each crystal are converted into pulse signals by a photomultiplier tube connected to a high voltage supply. The resulting output is passed through a preamplifier and amplifier combination. The amplified output from all four detectors is then mixed and routed into a single analogue channel, digitised, and stored as four consecutive 512 channel spectra on a PC based MCA (Canberra Industries Inc., S100 V 3.0, 1990). High voltage supplies are set at 560 volts and amplifier gains adjusted to ensure that amplified 10.83 MeV pulse signals fall within the upper quintile of the nominal zero-to-ten volt amplifier output range. Amplifier output pulses are also shaped with a 0.25 μsec time constant to minimise the count rate of randomly summed prompt γ-rays.[15] Furthermore, the lower level discriminator of the mixer-router is set to exclude pulse signals below 1.2 MeV from analysis; this reduces the spectroscopy system dead time to about 5%.

Spectral Analysis

A γ-ray spectrum from the measurement scan of a child (30 kg) is shown in figure 3. Energy calibration of spectra is performed using the distinctive photo peaks from hydrogen (2.22 MeV), chlorine (6.11 MeV) and lead (7.37 MeV).[17] The nitrogen, chlorine and hydrogen regions of interest (ROI) are defined as 9.4 - 11.1 MeV, 8.4 - 9.0 MeV and 2.0 - 2.4 MeV respectively. The spectral continuum beneath the hydrogen ROI is estimated as the region from 2.5 to 2.9 MeV. For each detector, this continuum is approximately a straight line with a negative gradient ranging from about 120 to 140 counts per channel for both subject and calibration phantoms alike. Furthermore, the variability of this gradient, as established over a 12 week period from 10 measurements of a child-size bottle phantom containing a urea-salt solution, is about 5% (CV) for each detector. Figure 3 also shows a background spectrum from a bottle phantom filled with water superimposed over the nitrogen and chlorine ROI's, and a hydrogen-background spectrum from an air phantom (obtained by irradiating an empty bed) superimposed over the hydrogen ROI (see 'Hydrogen Region of Interest'). Gross counts from nitrogen, chlorine and hydrogen are obtained by integration over the respective ROI's.

Nitrogen Region of Interest

We studied the effect of body elements, other than nitrogen, on background in the nitrogen ROI by measuring three bottle phantoms (each 28 cm × 14 cm × 30 cm) containing 10 litres of either plain water, a saline solution (0.14% Cl by weight) or a nitrogen-free, tissue-equivalent solution (9.2% H, 0.11% Cl, 1.1% Ca, 0.15% K, 26.9% C and 1.1% P by weight; determined from Chettle *et al*[18]). Our investigations revealed no significant contribution to the nitrogen background by either the chlorine or the nitrogen-free, tissue-equivalent solution. A subject's true nitrogen count ($N_{c\,sub}$) is therefore determined as

$$N_{c\,sub} = G^{N}_{sub} - B^{N}_{water} \qquad (3)$$

where G^{N}_{sub} is the gross counts in the nitrogen ROI of the subject spectrum, and B^{N}_{water} is the width and thickness corrected background counts over the same region determined from a spectrum of a plain water phantom (see 'Measurement Protocol', step 4). These findings contrast with other studies[15,6,19] which demonstrate nitrogen background to be effected by the random summing of γ-rays from chlorine and from other γ-rays in the 4 to 7 MeV range. This contrast may be explained by the observation that the random-summing count rate is dependant on neutron-source strength[15] and that other facilities use relatively stronger neutron sources (Melbourne,

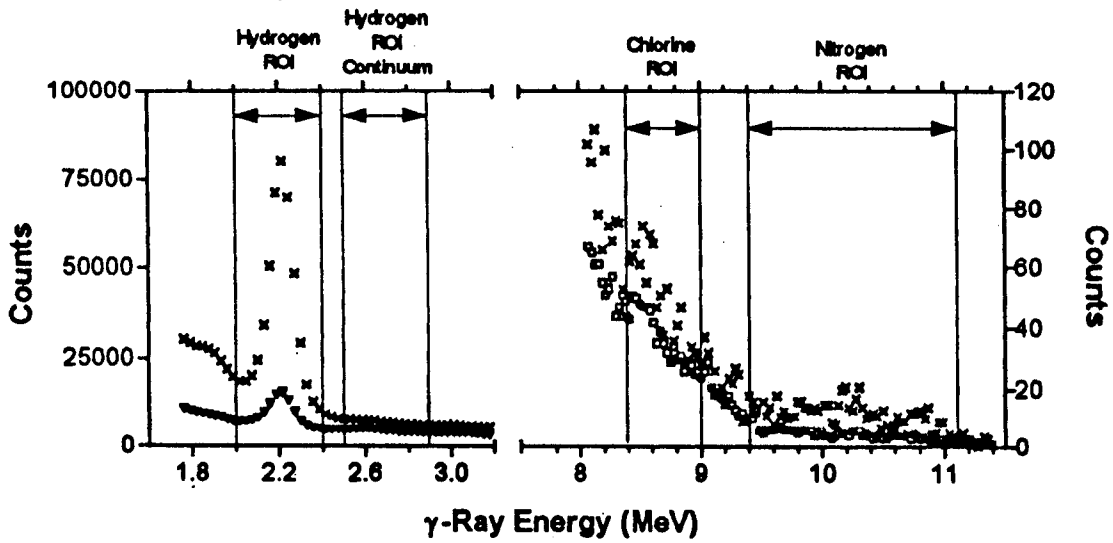

Figure 3. *γ-ray spectra from one 10 cm × 10 cm × 15 cm NaI(Tl) detector showing counts from a child subject (×) (600 s live time), water-phantom background counts in the nitrogen and chlorine ROI's ( ), and air-phantom counts in the hydrogen ROI and hydrogen-ROI continuum (▽); all phantom counts are scaled to a subject-scan live time of 600 sec (see 'Measurement Protocol').*

present study: 0.2 GBq ^{252}Cf with 2.3 × 10^7 n/s yield at ~2.2 MeV/n; Toronto, McNeill *et al*[15]: 2 x 370 GBq ^{238}Pu/Be with 5.8 × 10^7 n/s yield at ~3.5 MeV/n; Auckland, Mitra *et al*[8]: 2 × 282GBq ^{238}Pu/Be with 4.4 × 10^7 n/s yield at 3.5 MeV/n; Leeds Yankuba *et al*[19]: 14 MeV (d,T) neutron generator with ~10^9 n/s output).

Chlorine Region of Interest

In principle, possible causes of chlorine background include the detection of non-chlorine γ-rays within the chlorine ROI, the compton scattering of γ-rays from above the chlorine ROI and the random summing of γ-rays from below the chlorine ROI. An investigation of these factors yielded three outcomes. First, using the reference data of Lone *et al*[17], it was concluded that no body element, other than chlorine, produces a significant count-rate of prompt γ-rays within the chlorine ROI. Second, only nitrogen emits a significant count rate of γ-rays above the chlorine ROI. This results in a significant count rate of compton scattered 10.83 MeV γ-rays in the chlorine ROI (B^{Cl}_{compt}). In practice, B^{Cl}_{compt} represents a proportion of the subject's true nitrogen count and is calculated as the product of $N_{c\ sub}$ (equation 3) and the ratio of the true nitrogen counts in the chlorine ROI to the true nitrogen counts in the nitrogen ROI from a spectrum of a standard urea solution (10.3% N by weight, 'Measurement Protocol', step 5). This ratio is determined each time the facility is calibrated and is found, from subsidiary experiments, to be independent of nitrogen concentration over a range from 0.1% to 10.3% (by weight) and independent of both phantom width and thickness. Third, we investigated the effect on chlorine background of randomly summed γ-rays from major body elements other than chlorine and nitrogen by measuring two bottle phantoms (each 28 cm × 14 cm × 30 cm), one containing plain water (10 litre) and the other a chlorine-and-nitrogen-free, tissue-equivalent solution (9.2% H, 1.1% Ca, 0.15% K, 26.9% C and 1.1% P by weight; volume: 10 litre). We observed no significant difference in chlorine background between the water phantom and the chlorine-and-nitrogen-free, tissue-equivalent phantom. These observations however do not exclude the possibility of counts arising in the chlorine ROI from the random summing of 6.11 MeV γ-rays from chlorine and 2.22 MeV γ-rays from hydrogen. Although the summed energy is below the chlorine ROI, the limited detector resolution does not preclude some overlap. This potential effect, however, is not likely to compromise the final chlorine measurement as this effect is associated with chlorine itself. A subject's true chlorine count ($Cl_{c\,sub}$) is therefore determined as

$$Cl_{c\,sub} = G^{Cl}_{sub} - B^{Cl}_{water} - B^{Cl}_{compt} \qquad (4)$$

where G^{Cl}_{sub} is the gross counts in the chlorine ROI of the patient spectrum, B^{Cl}_{water} the width and thickness corrected background counts over the same region in a spectrum from plain water ('Measurement Protocol', step 4), and B^{Cl}_{compt} the compton-scattered 10.83 MeV prompt γ-rays in the chlorine ROI of the patient spectrum.

Hydrogen Region of Interest

A primary source of hydrogen background is neutron-activated γ-rays from hydrogen nuclei within the irradiation and detection components of the facility. In practice, hydrogen background is determined from a static scan of the bed alone (air phantom) and is calculated as the integral over the hydrogen ROI (G^H_{air}) less an estimate of the spectral continuum beneath the 2.22 MeV photo-peak defined as the integral from 2.5 to 2.9 MeV (B^H_{air}). Similarly, hydrogen counts from a subject spectrum are calculated as the integral over the hydrogen ROI (G^H_{sub}) less the integral over the 2.5 to 2.9 MeV region (B^H_{sub}). The subject's true hydrogen count ($H_{c\ sub}$) is therefore

$$H_{c\ sub} = \left(G^H_{sub} - B^H_{sub}\right) - \left(G^H_{air} - B^H_{air}\right) \qquad (5)$$

At MMC, hydrogen counts from the facility expressed as a proportion of the total hydrogen counts from the subject spectrum (i.e. $[G^H_{air} - B^H_{air})/(G^H_{sub} - G^H_{sub}]$) typically ranges from about 18% for children (≈30 kg) down to about 10% for adults (≈100 kg). In comparison, other authors have determined the hydrogen-background component of subject spectra using D_2O filled phantoms and comparable irradiation-detection geometries. Humphries *et al*[20] report that hydrogen background as a proportion of the hydrogen counts from subject spectra ranges from about 13% for children (≈22 kg) down to about 9% for adults (99 kg) whilst Baur *et al*[5] report this proportion to range from 1-4% for child-like masses. Notably, the impact of the relative size and variation of hydrogen background on estimates of TBN and TBCl in child-like masses is less than or comparable to the natural variability of the IVNAA method.[20] This apparent insensitivity arises because, as a transposition of equation 1 shows, values of TBN and TBCl are determined from the product of the ratio of hydrogen counts from the calibration phantom to that from the subject and the reciprocal of this ratio as expressed in the attenuation correction factor A (i.e. $(H_{c\ cal}/H_{csub})\times(H_{c\ sub}/H_{c\ cal})_{phant}$). This product is relatively insensitive to the accuracy and variability of hydrogen-background estimates.

Calibration and Performance Characteristics of the Prompt-γ IVNAA Facility

Effect of Body Size on Nitrogen and Chlorine Background

We investigated the effect of body width and thickness on background measurements in both the nitrogen and chlorine ROI's using water-filled bottle phantoms of varying width (16 cm, 24 cm, 32 cm, 40 cm, 48 cm) and thickness (8 cm, 16 cm, 24 cm, 32 cm). Figure 4a shows a series of second order polynomials relating nitrogen background to both phantom width and thickness. On one hand, nitrogen background clearly increases with phantom-width values between 16 cm to 32 cm, and peaks in the 30 cm to 40 cm phantom-width range. Furthermore, nitrogen background decreases with phantom-width values between 30 cm to 48 cm. On the other hand, the relationship between nitrogen background and phantom thickness is not as clearly resolved from the natural variability of background counts. However, figure 4a does suggest that for relatively narrow (width ≤ 24 cm) or wide (width ≈ 48 cm) phantoms, nitrogen background respectively increases or decreases with thickness. Overall, we observe a relatively stronger dependence of nitrogen background on phantom width than on thickness.

Figure 4b shows the relationship between chlorine background and both phantom width and thickness as series of second order polynomials similar to that observed for nitrogen background. Chlorine background is clearly related to phantom width, with maximum chlorine-background values observed between phantom widths of 20 cm and 40 cm. Figure 4b also suggests that chlorine background is related to phantom thickness, this effect being most significant for extreme phantom widths (viz. 16 cm and 48 cm).

The relationships shown in figure 4 reflect the irradiation-detection geometry particular to the MMC IVNAA facility and may be explained by the fact that a significant component of background is due to the random summing of prompt γ-rays from below the nitrogen and chlorine ROI's that result from neutron capture by elements such as hydrogen, lead, aluminium, sodium and iodine present in the facility.[15,21] As the size of a small phantom increases, the number of neutrons scattered into the detectors and surrounding materials also increases. This effect increases the random-summing count rate and hence background. As phantom dimensions become relatively large, neutrons and γ-rays become increasingly absorbed by the phantom. This effect decreases the random-summing count rate and hence background. Studies performed at other facilities using irradiation-detection geometries similar to that used at MMC also show nitrogen background to be related with both phantom width and thickness[22,23,13] or phantom width alone.[5]

Effect of Body Size on N_c/H_c and Cl_c/H_c Count Ratios

We investigated the effect of differential attenuation of 10.83 MeV, 8.57 MeV and 2.22 MeV γ-rays in body tissue by measuring N_c/H_c and Cl_c/H_c count ratios from bottle phantoms of varying width (16 cm, 24 cm, 32 cm, 40 cm, 48 cm) and thickness (8 cm, 16 cm, 24

cm, 32 cm) filled with either a urea solution (5.1% N by weight) or saline solution (0.57% Cl by weight). Background corrections in the nitrogen and chlorine regions were determined from identical phantoms filled with plain water whilst hydrogen background was determined from an air phantom. Each phantom type and geometry was irradiated once over a 3600 s live-time period.

Figure 5 shows the linear regressions of N_c/H_c and Cl_c/H_c versus phantom width for a series of phantom thicknesses. Clearly, N_c/H_c and Cl_c/H_c demonstrate a primary dependence on phantom width and a secondary dependence on phantom thickness. These results compare with reports from other facilities based on similar irradiation-detection geometries which show N_c/H_c to be related with width,[5,22] and Cl_c/H_c to be related with both width and thickness.[6] Furthermore, it should be noted that, because hydrogen background was not measured explicitly as a function of phantom width and thickness, figure 5 represents the effects of both differential attenuation of corporeal 10.83 MeV, 8.57 MeV and 2.22 MeV γ-rays and the attenuation of hydrogen background.

The effect on N_c/H_c of a subject's departure in width and thickness from the dimensions of the standard-size calibration phantom (28 cm width × 14 cm thickness, 'Measurement Protocol', step 5) was determined from the data in figure 5a as the ratio of N_c/H_c for the calibration-phantom width and thickness to that of N_c/H_c for the subject's average width and thickness ('Measurement Protocol', step 3). This ratio represents a γ-ray attenuation correction factor A which is determined empirically as

$$A = 1/[\,0.769 + 0.00865 \times \text{width} + 0.00173 \times (\text{thickness} - 20)] \quad (6)$$

where the width dependant term is derived from the line of best fit to the mean N_c/H_c count ratio at each phantom width ($r = 0.999$, $P < 0.0001$), and the thickness dependant term derived by calculating the mean N_c/H_c difference per centimetre thickness at each phantom width. Notably, equation 6 shows that, for a given subject width and thickness, the attenuation correction applied to N_c/H_c is about 0.9% per 1 cm increment in width and about 0.2% per 1 cm increment in thickness relative to the calibration-phantom dimensions. The attenuation-correction factor for Cl_c/H_c was also determined and found to be very similar to equation 6. This is not surprising because the attenuation coefficients for 8.57 MeV and 10.83 MeV γ-rays in body tissue are similar ($0.024cm^{-1}$ versus $0.022cm^{-1}$ respectively).

The correction factors determined in this study compare favourably with other centres that use similar IVNAA facility geometry. In particular, McNeill *et al*[24] has applied a 1% correction per centimetre thickness to N_c/H_c, whilst the work of Mackie *et al*[25] shows implicitly a correction of about 1% per centimetre width applied to N_c/H_c. In addition, Beddoe *et al*[25] has also reported a dependency between Cl_c/H_c (counting 6.11 MeV prompt γ rays from Cl) and phantom width which amounts to a correction of about 2% per centimetre width.

Linearity of Measurement Response

The linearity of measurement of both N_c/H_c and Cl_c/H_c was determined from spectra of bottle phantoms of constant volume containing either a urea or saline solution of varying concentrations. Nitrogen concentrations ranged from one-half through to four times physiological concentration (i.e. 1.3% - 10.3% by weight). Chlorine concentrations ranged from one-half through to eight times physiological concentration (i.e. 0.071% - 1.14% by weight). These ranges include the elemental concentrations found in children (2.3% N and 0.13% Cl by weight[26,27]) and in the calibration phantoms (i.e. 10.3% N and 1.14% Cl by weight). Linear regression analysis of both Nc/Hc and Cl_c/H_c versus respective concentrations of nitrogen and chlorine revealed a very good linear measurement response (N:$r^2 = 0.9989$, SEE = 2.4%, $P<0.0001$; Cl:$r^2 = 0.9996$, SEE = 1.2%, $P<0.0001$; SEE: standard error of estimating Y divided by $\bar{y}$).

Measurement Protocol

The measurement protocol at MMC determines absolute estimates of TBN and TBCl using the relation detailed in equation 1. The variables in equation 1 are described and determined by the following steps:

1). To account for the variability of TBH with growth, maturation and health status in children, TBH is determined using a four compartment model of body weight (BW) defined as the sum of total body water (TBW) as measured by the D_2O dilution technique, TBPr estimated by IVNAA as 6.25 × TBN, total body bone mineral (TBBM) determined by dual energy x-ray absorptiometry (DEXA), and fat mass (FM) calculated as body weight less the sum of TBW, TBPr, and TBBM. The known hydrogen content of water, protein and fat (respectively 11.1%, 7.0% and 12.0% by weight) is then used to calculate TBH as

$$TBH = 0.12 \times (BW - TBBM) - 0.0089 \times TBW - 0.05 \times TBPr \quad (7)$$

where the hydrogen content of TBBM and the glycogen content of BW is assumed to be negligible.[28,29] Equation 7 is then substituted into equation 1 to determined TBN. This method has been fully described by Beddoe *et al*.[22]

Figure 4a.

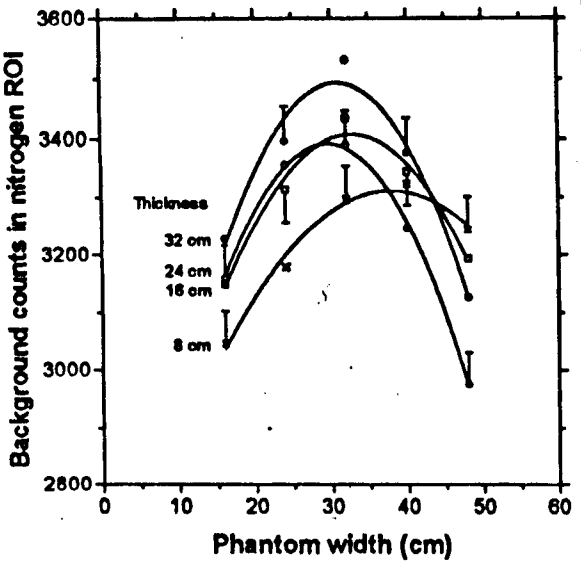

Figure 4b.

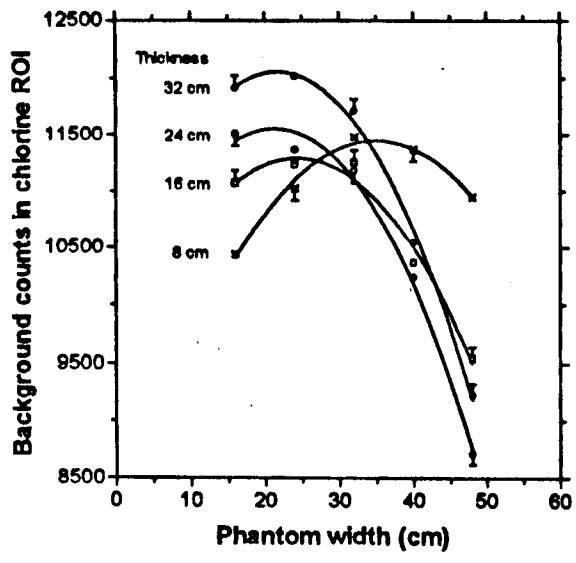

Figure 4. *Gross counts in the nitrogen region of interest (figure 4a) and chlorine region of interest (figure 4b) from 3600s (live time) static scans of water-filled bottle phantoms of different width and thickness; phantom thickness: (×) 8 cm; (□) 16 cm; (○) 24 cm; (●) 32 cm.*

2). The subject's N_c/H_c and Cl_c/H_c count ratios are measured by a 630 s scan (600 s live time) of the subject lying flat on a scanning bed. A uni-lateral irradiation is performed from shoulder to mid-thigh in three sections, namely, the chest, abdomen and the hip and mid-thigh region. Each section is irradiated for 105 s in both the supine and prone positions.

3). To correct for the effect of body size on background and γ-ray attenuation, the lateral width and the anterior-posterior thickness of the subject lying supine is measured at the chest, waist, hip and mid-thigh according to the standards of Lohman *et al.*[29] An average width and thickness is then determined using estimated volumes of each irradiated section as a weighting factor.

4). Width and thickness corrections for background variation are applied to the subject's N_c/H_c and Cl_c/H_c count ratios using an empirical relationship based on the data in figures 4a and 4b which relates nitrogen and chlorine background on the one hand, with both width and thickness on the other. A γ-ray attenuation correction A is also applied (equation (6)).

5). The calibration-phantom terms in equation 1 are determined from static irradiations of polyethylene-bottle phantoms of child-like dimensions measuring 28 cm (width) × 14 cm (thickness) × 60 cm (length) and containing either plain water, a urea solution (10.3% N and 10.6% H by weight) or NaCl solution (1.14% Cl and 11.3% H by weight). In particular, nitrogen and chlorine background is, in part, determined from a 3600 s (live time) water-phantom spectrum, TBN measurements are calibrated against a 2400 s live-time scan of the nitrogen phantom, TBCl measurements are calibrated against a 3600 s live-time scan of the chlorine phantom, and hydrogen background is determined from a 2400 s live-time static irradiation of an empty bed. Counts from all calibration spectra are then scaled to a subject-measurement live time of 600 s. All calibration measurements are performed on the same day as subject measurements.

Dosimetry

Equivalent fast-neutron (≈1 MeV) and γ-ray doses were respectively measured with a CR39 plastic-plaque dosimeter and a thermoluminescent dosimeter consisting of $CaSO_4$ impregnated with Dy respectively.[30] Both dosimeters were sealed in a single plastic badge of external dimensions 40 mm × 60 mm × 17 mm. The respective maximum errors of

measurement for the neutron and γ-ray dosimeters are ±30% and ±15%.[30]

The dose equivalent distribution as a function of subject depth was determined from a unilateral, static scan of a water phantom. In particular, one dosimeter badge was positioned on the scanning bed directly above the neutron source. A bottle phantom containing water and measuring 32 cm × 16 cm × 100 cm was then positioned centrally on the scanning bed over the dosimeter badge. A second dosimeter badge was placed on top of the phantom, directly over the neutron source. Table 1 shows the resulting dose-depth measurements per 630 s static irradiation. Equivalent doses are shown at phantom depths of 0 cm (entrance dose), 16 cm (exit dose) and 8 cm (i.e. the average of entrance and exit doses). Also shown is the average dose equivalent derived for a bilateral irradiation. The quality factors used for neutrons and γ-rays are 20 and 1 respectively.[31]

Table 1. *Dose equivalent depth distribution for a 630 s static irradiation of a water phantom.*

Height above bed level (cm)[a]	0	8	16
Dose Equivalent (mSv) (uni-lateral)[b]:			
H_γ	0.027	0.017	0.0068
H_n	1.16	0.72	0.29
H_{total}	1.19	0.74	0.30
Dose Equivalent (mSV) (bi-lateral):			
H_{total}	0.74	0.74	0.74

[a] Uni-lateral doses at 8 cm calculated as the average of measured values at 0 cm and 16 cm.
[b] H_γ - γ-ray dose equivalent (Q=1); H_n - neutron dose equivalent (Q=20); $H_{total} = H_\gamma + H_n$.

Based on the data in table 1, the total body effective dose equivalent rate is determined to be 0.74 mSv per 630 s bilateral irradiation. A 630 s measurement scan consisting of three juxtaposed exposures from shoulder to mid-thigh therefore results in an effective dose equivalent of 0.25 mSv. The health risk associated with this level of exposure in children is 1 in 10^5 which is described by the ICRP[16] as "minor to intermediate" and is justified if the radiation exposure leads to health benefits (e.g. an increase in knowledge). Moreover, this category of risk remains unchanged even when allowing for the ICRP statement that "the health risk per unit dose to children is 2 to 3 times greater than for adults (aged less than 50 years)".[16]

Facility Performance Appraisal

Precision and Accuracy of Measurement

The precision and accuracy of the method was determined from forty-eight measurements performed on fourteen separate days over a three month period using a child-size, polythene-bottle phantom weighing 34 kg, measuring 28 cm × 14 cm ×

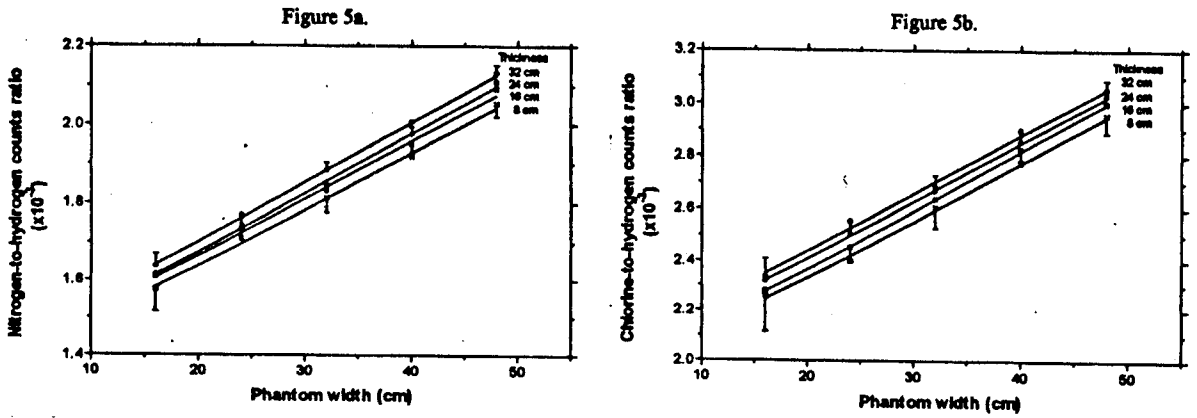

Figure 5. *Nitrogen-to-hydrogen counts ratio (N_c/H_c, figure 5a) and chlorine-to-hydrogen counts ratio (Cl_c/H_c, figure 5b) from 3600s (live time) scans of bottle phantoms of different width and thickness containing either a urea solution (5.1% N by weight) or saline solution (0.57% Cl by weight); phantom thickness: (×) 8 cm; (□) 16 cm; (○) 24 cm; (●) 32 cm; for all linear relationships, r = 0.999 and P<0.0001.*